Effects of strain on the electronic structures and T C 's of the La 0.67 Ca 0.33 Mn O 3 and La 0.8 Ba 0.2 Mn O 3 thin films deposited on Sr Ti O 3

Hsiung Chou, M.-H. Tsai, F. P. Yuan, S. K. Hsu, C. B. Wu, J. Y. Lin, C. I. Tsai, and Y.-H. Tang

Citation: Applied Physics Letters **89**, 082511 (2006); doi: 10.1063/1.2335973
View online: http://dx.doi.org/10.1063/1.2335973
View Table of Contents: http://scitation.aip.org/content/aip/journal/apl/89/8?ver=pdfcov
Published by the AIP Publishing

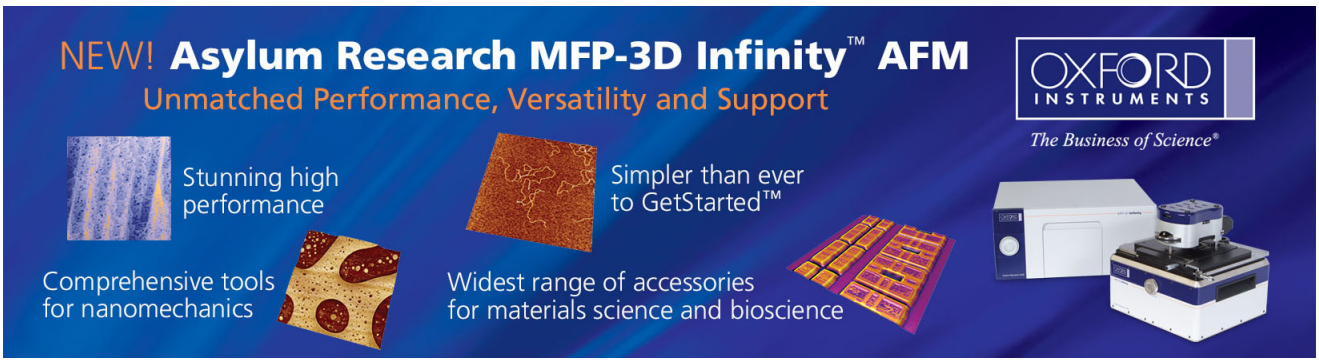

Effects of strain on the electronic structures and T_C's of the $La_{0.67}Ca_{0.33}MnO_3$ and $La_{0.8}Ba_{0.2}MnO_3$ thin films deposited on $SrTiO_3$

Hsiung Chou,[a] M.-H. Tsai, F. P. Yuan, S. K. Hsu, and C. B. Wu
Department of Physics, National Sun Yat-Sen University, Kaohsiung, Taiwan 804, Republic of China and Center for Nanoscience and Nanotechnology, National Sun Yat-Sen University, Kaohsiung, Taiwan 804, Republic of China

J. Y. Lin and C. I. Tsai
Institute of Physics, National Chiao Tung University, Hsinchu, Taiwan 300, Republic of China

Y.-H. Tang
Department of Physics, National Sun Yat-Sen University, Kaohsiung, Taiwan 804, Republic of China and Center for Nanoscience and Nanotechnology, National Sun Yat-Sen University, Kaohsiung, Taiwan 804, Republic of China

(Received 19 April 2006; accepted 5 July 2006; published online 24 August 2006)

The strain effects on the electronic structures of $La_{0.67}Ca_{0.33}MnO_3$ (LCMO) and $La_{0.8}Ba_{0.2}MnO_3$ (LBMO) thin films have been studied by O *K*-edge x-ray absorption near edge structure (XANES) spectroscopy. For LCMO, the first-principles calculations reveal that the features in the XANES spectra are associated with hybridized states between O $2p$ and Mn minority-spin $3d$ t_{2g} and e_g, La $5d$/Ca $3d$, and Mn $4s$/Ca $4p$ states. An analysis of these features shows that the tensile strain decreases substantially La–O and Ca–O hybridization and T_C for LCMO. For LBMO, the small compressive strain enhances slightly La–O and Ba–O hybridization and T_C. © *2006 American Institute of Physics*. [DOI: 10.1063/1.2335973]

Since the discovery of colossal magnetoresistance in $R_{1-x}A_xMnO_3$ (R=rare-earth ion and A=divalent ion) materials in 1950,[1–6] the metal-like (M)-insulator-like (I) transition temperature (T_p) and the ferromagnetic (F)-paramagnetic (P) transition temperature (T_C) of doped $R_{1-x}A_xMnO_3$ thin films have been found to be affected by the strain[7–15] due to lattice mismatch with the substrate. When $La_{1-x}Ca_xMnO_3$ (LCMO) was grown on $SrTiO_3$ (STO) (001) substrates by pulsed laser ablation, the larger lattice spacing of the substrate causes an in-plane tensile strain and a corresponding shrinkage along the out-of-plane axis in the films. The tensile strain was found to reduce T_C of LCMO films. In contrast, T_C of the ultrathin $La_{1-x}Ba_xMnO_3$ (LBMO) film was found to increase up to x=0.2 and then decrease beyond 0.2. The highest T_C reported for LBMO films was 310 K for x=0.2 with a thickness of 21 nm.[15]

Up to date, the different behavior between LCMO and LBMO has not been well understood. Kanki *et al.*[14] and Zhang *et al.*[15] proposed a $d_{x^2-y^2}$ orbital stability model based on the elongation of the in-plane Mn–O bond length to explain the enhancement of T_C in thin LBMO films. However, the elongation of a bond usually results in a weakening of the bond strength. Based on extended x-ray absorption fine structure and high-resolution x-ray diffraction measurements, Miniotas *et al.*[16] observed that the Mn–O bond length is fixed for LCMO deposited either on STO or $LaAlO_3$. Yuan[17] also questioned the interpretation of Mn–O bond elongation in LBMO thin films by Zhang *et al.*[15] and argued that the enhancement of T_C could be due to strain-induced alteration of the Mn–O–Mn bond angles.

In this study, the O *K*-edge x-ray absorption near edge structure (XANES) technique, which is a powerful tool to elucidate changes of electronic structures associated with the alteration of the bonding environment of O ions, is employed to study ultrathin and thick LCMO and LBMO films to better understand the effects of lattice-mismatch induced strain on the electronic structures and T_C's of these two manganites.

LCMO (x=0.33) and LBMO (x=0.2) thin films were grown on STO (001) single crystal substrates by an off-axis rf magnetron sputtering system. The LCMO films with thicknesses of 200 and 20 nm and the LBMO films with thicknesses of 150 and 15 nm were deposited at substrate temperatures of 750 and 800 °C, respectively, followed by an *in*

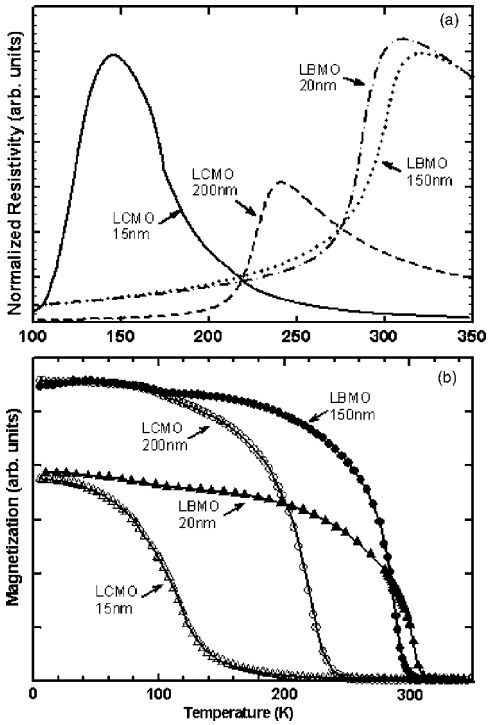

FIG. 1. Normalized R-T (a) and M-T (b) curves of 200- and 20-nm-thick LCMO films and 150- and 15-nm-thick LBMO films.

[a]Electronic mail: hchou@mail.nsysu.edu.tw

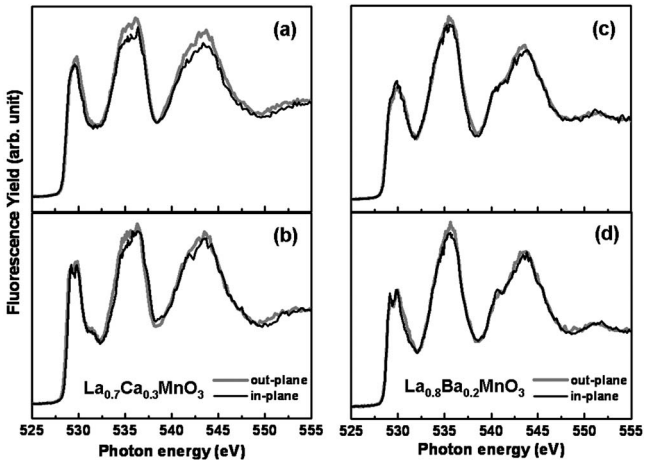

FIG. 2. O *K*-edge XANES spectra in the fluorescence yield mode of the 200-nm-thick LCMO film taken at (a) room temperature and (b) 30 K. O *K*-edge XANES spectra of the 50-nm-thick LBMO film were taken at (c) room temperature and (d) 30 K.

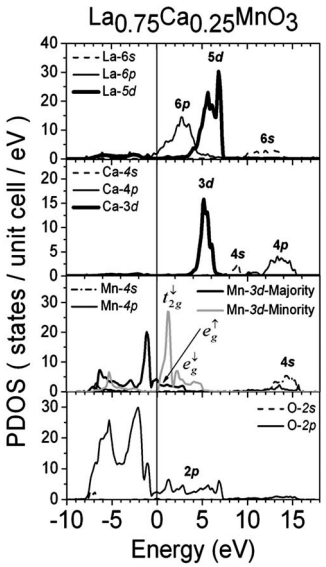

FIG. 3. Partial densities of states (PDOSs) for La, Ca, Mn, and O ions in $x=1/4$ LCMO.

situ annealing at 850° C for 2 h in 500 Torr pure oxygen. The crystal structures and transport properties have been studied by x-ray diffraction and four-point probe measurements, respectively. The superconducting quantum interference device by Quantum Design was used to measure magnetization. The O *K*-edge XANES spectra were taken using the high-energy spherical grating monochromator beamline at the Synchrotron Radiation Research Center (SRRC) in Taiwan, operating at 1.5 GeV with a maximum stored current of 200 mA. The spectra were taken using the fluorescence yield (FY) and total electron yield (TEY) modes at room temperature ($T=300$ K) and low temperature ($T=30$ K) in a vacuum better than 1×10^{-9} Torr. The energy resolution of the monochromator is around 0.1 eV. The background and the self-absorption effects of spectra were subtracted and corrected by the standard procedure. The final spectra were then normalized to the tabulated standard absorption cross section in the energy range between 600 and 620 eV.

The resistivity and magnetization curves of the films shown in Fig. 1 have typical $F\rightarrow P$ and $M\rightarrow I$ transitions around the Curie temperatures T_C and the resistivity-peak temperatures T_p. The 200-nm-thick LCMO film behaves bulklike (with a T_C of 242 K and a T_p of 235 K). T_C and T_p of the 20-nm-thick LCMO film, however, are reduced by 40% and 36% down to 146 and 146 K, respectively. The correlated reduction of T_C and T_p suggests that $F\rightarrow P$ and $M\rightarrow I$ transitions may have the same origin. The drastic reduction of T_C and T_p can be attributed to the localization effect of Mn $3d$ majority-spin (↑-spin) e_g orbitals, since the F property of LCMO was found to be due to Ca induced delocalization of O $2p$ and Mn $3d$ ↑-spin e_g states near the Fermi level E_F.[18] The tensile strain may induce weakening of the Ca–O hybridization and reduce the density of delocalized Mn ↑-spin e_g states and consequently T_C and T_p.

The 150-nm-thick LBMO film has T_C and T_p of 296 and 312 K, respectively, while both T_C and T_p are enhanced to 311 and 330 K by 5% and 6%, respectively, for the 15-nm-thick film. This tendency is opposite to that of LCMO. The differences between LBMO and LCMO are that the Ba ion is much larger than Ca and La ions and that Ba has a lower electronegativity.[19] The STO substrate has a lattice constant of $a=3.905$ Å.[20] Along the [110] direction, the periodicity is $\sqrt{2}a=5.523$ Å, which is greater and smaller than the a lattice constants of 5.4572 Å for LCMO (Ref. 21) and 5.544 45 Å for LBMO,[22] respectively. Thus, the ultrathin LCMO and LBMO films have in-plane tensile and compressive strains, respectively, and have opposite behavior of the changes of T_C and T_p. The compressive strain is expected to increase hybridization between Ba and O orbitals and consequently the increase of the Ba induced delocalization of Mn $3d$ ↑-spin e_g and O $2p$ orbitals.

Since FY O *K*-edge XANES measures bulk electronic structures, the substrate contribution overshadows those of ultrathin films, spectra were taken for thick films only. The incident angles of the x-ray beam were chosen to be 0° (normal) and 60° (oblique). Figure 2 show spectra of LCMO and LBMO films at room temperature and 30 K, respectively. And Fig. 3 shows the partial densities of states (PDOSs) of the various ions for $x=1/4$ LCMO obtained by spin-polarized first-principles pseudofunction method.[23] Comparison between Figs. 2 and 3 identifies that the leading twin-peak feature at ~529 eV is contributed by hybridized states between O $2p$ and Mn $3d$ ↓-spin t_{2g} and e_g states. The La $6p$ band also contributes to the spectra in the same energy region. The peaks of Mn $3d$ ↓-spin t_{2g} and e_g subbands and the unoccupied part of the O $2p$ band are separated by ~0.1 eV in good agreement with that of the twin peaks in the 30 K spectra of LCMO. The two other features centered at ~6.5 and ~14 eV above the leading feature can be identified to be the hybridized states between O $2p$ and La $5d$/Ca $3d$ states at ~5 eV and Mn $4s$/Ca $4p$ states at ~13 eV, respectively. The agreement between calculation and experiment is reasonably good. Note that the assignments of these three features are different from those proposed earlier.[24–29] The spectra of LBMO also have three major features similar to those of LCMO.

The intensities of the second and third features in the room-temperature O *K*-edge XANES spectrum of LCMO with the 0° incident angle (out-of-plane direction) are higher than those with the 90° angle (in-plane direction). This anisotropy is decreased at 30 K. The anisotropy is much less significant and less temperature-dependent for LBMO. The present results suggest that the in-plane tensile and out-of-

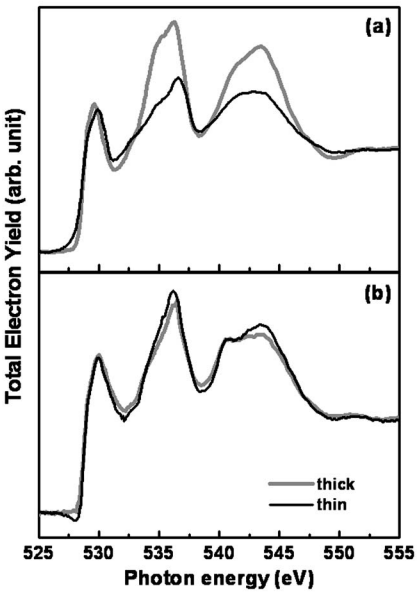

FIG. 4. O *K*-edge XANES spectra of (a) LCMO and (b) LBMO films taken at room temperature in the total electron yield mode.

plane compressive strains near the LCMO/STO interface region cause enhancement and reduction of the densities of Ca $3d4p$/La $5d$ states, respectively.

The TEY O *K*-edge XANES probes dominantly top layers of the film and is used to investigate the differences in the electronic structures of strained ultrathin and relaxed thick LCMO and LBMO films. The TEY spectra are shown in Fig. 4. The intensities of the leading features for the LCMO and LBMO films are insensitive to the thickness, or the strain, while the intensities of the second and third features for the strained ultrathin LCMO film drop by about half from those of the unstrained thick film. In contrast, the intensities of the second and third features for the strained ultrathin LBMO film are slightly enhanced relative to those of the unstrained thick film. Since the leading feature and the second and third features are contributed by O $2p$/Mn $3d$ $\downarrow$-spin t_{2g} and e_g hybridized states, O $2p$/La $5d$/Ca $3d$ hybridized states, and Mn $4s$/Ca $4p$ states, respectively, the intensity trend for LCMO suggests that the tensile strain weakens substantially the La–O and Ca–O hybridization, but does not significantly affect the relatively localized Mn 3d–O $2p$ hybridization. Note that the higher-energy Mn $4s$ state is delocalized, so that it may be also affected. The opposite and less significant changes of the intensities of the second and third features for LBMO are due to that the strain is compressive and that the lattice mismatch is much smaller, respectively.

In summary, a combination of FY and TEY O *K*-edge XANES measurements for LCMO and LBMO ultrathin and thick films deposited on the STO substrate and spin-polarized first-principles calculation for LCMO suggest that the tensile strain in the ultrathin LCMO film weakens substantially the hybridization between O $2p$ and La $5d$/Ca $3d4p$/Mn $4s$ states and decreases T_C, while the compressive strain in the ultrathin LBMO film enhances slightly the hybridization between O $2p$ and La $5d$/Ba $5d6p$/Mn $4s$ states and increases slightly T_C. The relatively localized O $2p$–Mn $3d$ $\downarrow$-spin t_{2g} and e_g hybridization is insensitive to the strain for both LCBO and LBMO.

This work was supported by the NSC Core Facilities Laboratory in Kaohsiung-Pingtung Area and by the National Science Council of Taiwan with Contract No. NSC 94-2120-M-110-002.

[1]G. Jonker and J. van Santen, Physica (Amsterdam) **16**, 337 (1950).
[2]J. van Santen and G. Jonker, Physica (Amsterdam) **16**, 559 (1950).
[3]M. Imada, A. Fujimori, and Y. Tokura, Rev. Mod. Phys. **70**, 1039 (1998).
[4]Y. Tokura and Y. Tomioka, J. Magn. Magn. Mater. **200**, 1 (1999).
[5]E. L. Nagaev, Phys. Rep. **346**, 387 (2001).
[6]E. Dagotto, T. Hotta, and A. Moreo, Phys. Rep. **344**, 1 (2001).
[7]S. Jin, T. H. Tiefel, M. McCormack, H. M. O'Bryan, L. H. Chen, R. Ramesh, and D. Schurig, Appl. Phys. Lett. **67**, 557 (1995).
[8]J. O'Donnell, M. S. Rzchowske, J. N. Eckstein, and I. Bozovic, Appl. Phys. Lett. **72**, 1775 (1998).
[9]S. Freisem, A. Brockhoff, D. G. de Groot, B. Dam, and J. Arats, J. Magn. Magn. Mater. **165**, 380 (1997).
[10]E. Gommert, H. Cerva, J. Wecker, and K. Samwer, J. Appl. Phys. **85**, 5417 (1999).
[11]F. Tsui, M. C. Smoak, T. K. Nath, and C. B. Eom, Appl. Phys. Lett. **76**, 2421 (2000).
[12]Vengalis, A. Maneikis, F. Anisimovas, R. Butkute, L. Dapkus, and A. Kindurys, J. Magn. Magn. Mater. **211**, 35 (2000).
[13]J. O'Donnell, M. Onellion, M. S. Rzchowski, J. N. Eckstein, and I. Bozovic, Phys. Rev. B **54**, R6841 (1996).
[14]T. Kanki, H. Tanaka, and T. Kawai, Phys. Rev. B **64**, 224418 (2001).
[15]J. Zhang, H. Tanaka, T. Kanki, J.-H. Choi, and T. Kawai, Phys. Rev. B **64**, 184404 (2001).
[16]A. Miniotas, A. Vailionis, E. B. Svedberg, and U. O. Karlsson, J. Appl. Phys. **89**, 2134 (2001).
[17]Q. Yuan, Phys. Rev. B **70**, 066401 (2004).
[18]M.-H. Tsai, Y.-H. Tang, H. Chou, and J. B. Wu, e-print cond-mat/0604367 and the bottom two panels shown in Fig. 4 of this study.
[19]*Table of Periodic Properties of the Elements*, (Sargent-Welch Scientific Company, Skokie, IL, 1980).
[20]R. H. Mitchell, A. R. Chakhmouradian, and P. M. Woodward, Phys. Chem. Miner. **27**, 583 (2000).
[21]S. J. Hibble, S. P. Cooper, A. C. Hannon, I. D. Fawcett, and M. Greenblatt, J. Phys.: Condens. Matter **11**, 9221 (1999).
[22]V. A. Cherepanov, E. A. Filonova, V. I. Voronin, and I. F. Berger, J. Solid State Chem. **153**, 205 (2000).
[23]R. V. Kasowski, M.-H. Tsai, T. N. Rhodin, and D. D. Chambliss, Phys. Rev. B **34**, 2656 (1986).
[24]M. Abbate, F. M. F. de Groot, J. C. Fuggle, A. Fujimori, O. Strebel, F. Lopez, M. Domke, G. Kaindl, G. A. Sawatzky, M. Takano, Y. Takeda, H. Eisaki, and S. Uchida, Phys. Rev. B **46**, 4511 (1992).
[25]M. Abbate, G. Zampieri, F. Prado, A. Caneiro, and A. R. B. de Castro, Solid State Commun. **111**, 437 (1999).
[26]E. Pellegrin, L. H. Tjeng, F. M. F. de Groot, R. Hesper, G. A. Sawatzky, Y. Moritomo, and Y. Tokura, J. Electron Spectrosc. Relat. Phenom. **86**, 115 (1997).
[27]J.-H. Park, T. Kimura, and Y. Tokura, Phys. Rev. B **58**, R13330 (1998).
[28]O. Toulemonde, F. Millange, F. Studer, B. Raveau, J.-H. Park, and C.-T. Chen, J. Phys.: Condens. Matter **11**, 109 (1999).
[29]N. Mannella, A. Rosenhahn, M. Watanabe, B. Sell, A. Nambu, S. Ritchey, E. Arenholz, A. Young, Y. Tomioka, and C. S. Fadley, Phys. Rev. B **71**, 125117 (2005).